Activity-based protein profiling in drug-discovery

Esbroeck, A.C.M. van

5

Identification of ABHD6 as a diacylglycerol lipase

A.C.M. van Esbroeck
X. Di
V. Kantae
T. van der Wel
H. den Dulk
A.T. Bakker
B.I. Florea
H.S. Overkleeft
T. Hankemeier
M. van der Stelt

ABSTRACT | The endocannabinoid 2-arachidonoyl-glycerol (2-AG) is an important signaling lipid, which is involved in neuronal differentiation. This study aimed to identify the biosynthetic enzymes responsible for 2-AG production during retinoic acid (RA)-induced neurite outgrowth of Neuro-2a cells, a widely used cellular model for neuronal differentiation. First, it was confirmed that RA stimulation of Neuro-2a cells led to 2-AG production and neurite outgrowth. The diacylglycerol lipase (DAGL) inhibitor DH376 abolished 2-AG levels and delayed neuronal differentiation. Surprisingly, CRISPR/Cas9-mediated knockdown of the 2-AG producing enzymes DAGLα and DAGLβ in Neuro-2a cells did not reduce cellular 2-AG levels, suggesting there are other enzymes capable of producing 2-AG in this cell line. Chemical proteomics revealed DAGLβ and α,β–hydrolase domain containing protein (ABHD6) as the only targets of DH376 in Neuro-2a cells. Biochemical, genetic and lipidomic studies demonstrated that ABHD6 possesses diacylglycerol lipase activity in conjunction with its previously reported role as monoacylglycerol lipase. RA treatment of Neuro-2a cells resulted in a three-fold increase in ABHD6 activity, whereas DAGLβ activity was decreased. Thus, these data extend the role of ABHD6 as a MAG lipase to a DAG lipase and suggest it is involved in neuronal differentiation.

Manuscript in preparation

Introduction

The endocannabinoid 2-archidonoylglycerol (2-AG) is an important signaling lipid in the central nervous system (CNS). It acts as a retrograde messenger that activates the presynaptic cannabinoid receptor type 1 (CB1R), thereby regulating neurotransmitter release. 2-AG is involved in a variety of physiological processes, including modulation of memory, energy balance and emotional states, such as stress and anxiety[1]. Biochemical, pharmacological and genetic studies have established diacylglycerol lipases α and β (DAGLα, DAGLβ) as the main biosynthetic enzymes that produce 2-AG in the brain by catalyzing the *sn*-1-specific hydrolysis of diacylglycerol (DAG) to generate 2-AG[2] (Figure 1). For example, congenital deletion of DAGLα or DAGLβ resulted in 80% and 50% reduction, respectively, of brain 2-AG levels in knockout (KO) mice as compared to wildtype (WT) littermates[3]. Pharmacological studies with covalent, irreversible, dual DAGL inhibitors, such as DH376 and DO34, showed that acute blockade of 2-AG biosynthesis in the mouse brain reduced neuroinflammatory responses[4], reversed LPS-induced anapyrexia[4], reduced food intake[5] and modulated cocaine-seeking behavior[6] and stress responses[7].

The life span of 2-AG signaling at the synapse is tightly controlled. Monoacylglycerol lipase (MGLL)[8] and α,β-hydrolase domain containing protein 6 and 12 (ABHD6, ABHD12) have been identified as the key enzymes terminating the physiological role of 2-AG. They hydrolyze the ester bond in 2-AG, thereby generating glycerol and arachidonic acid (AA)[9,10] (Figure 1). MGLL is the predominant lipase in the brain covering over 85% of 2-AG hydrolysis, whereas ABHD6 and ABHD12 account for 4 and 9%, respectively[11].

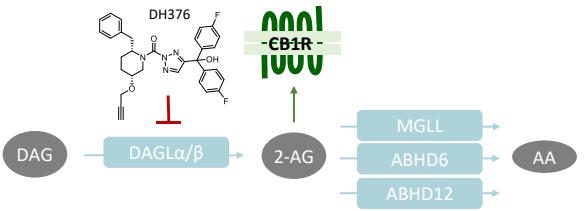

Figure 1 | Schematic overview of 2-AG signaling and metabolism. CB1R: Cannabinoid receptor type 1, DAGL: diacylglycerol lipase, MGLL: monoacylglycerol lipase, ABHD: α,β-hydrolase domain containing protein, DAG: diacylglycerol, 2-AG: 2-arachidonoyl glycerol, AA: arachidonic acid.

2-AG signaling is not only important in the adult brain, but multiple studies have also provided evidence of a functional role of 2-AG during neural developmental processes[12], including axonal growth and guidance[2,13–15], differentiation[16], and neurogenesis[3,17]. In adult mice, DAGLα is mainly restricted to postsynaptic sites on neurons, whereas DAGLβ is expressed in microglial cells, but during neuronal development their expression pattern is different. Both DAGLα and DAGLβ were found in neurons at developing axonal tracts[2,14,17,18]. Jung and colleagues have investigated the role of DAGLs in neuronal differentiation using retinoic acid (RA)-induced neurite outgrowth in murine neuroblastoma cell line Neuro-2a[16]. They found that RA elevated cellular 2-AG levels in Neuro-2a cells during differentiation and recombinant expression of DAGLα or DAGLβ

increased neurite outgrowth, whereas silencing the expression of DAGLs using shRNAs reduced the number of cells with neurites[16]. The contribution of the endogenously expressed DAGL enzymes to 2-AG biosynthesis in these cells is, however, less clear.

Here, we sought to revisit this question and aimed to dissect the role of the two DAGL isoforms in 2-AG biosynthesis in Neuro-2a using pharmacological and genetic methods. Surprisingly, CRISPR/Cas9-mediated knockdown (KD) of DAGLα and/or DAGLβ did not reduce 2-AG levels in Neuro-2a, suggesting that other enzymes contribute to 2-AG biosynthesis in these cells. Interestingly, treatment of the cells with the DAGL inhibitor DH376 almost completely abolished cellular 2-AG levels. Chemical proteomics of DH376-treated Neuro-2a revealed ABHD6 as the only other target of DH376. Additional biochemical, genetic and lipidomics studies showed that ABHD6 possesses diacylglycerol lipase activity, next to its previously reported role as monoacylglycerol (MAG) lipase. The identification of ABHD6 as a general lipase using both DAGs and MAGs as substrates, may have important implications for its proposed role in the endocannabinoid system.

Results & Discussion

To investigate the role of DAGL in neuronal differentiation, Neuro-2a cells were incubated with RA, which induced a time-dependent outgrowth of neurites (Figure 2A-B). This was accompanied by increased cellular 2-AG levels as determined by liquid chromatography-mass spectrometry (LC-MS) (Figure 2C). These findings confirm the results of Jung *et al.*[16]. Of note, anandamide (AEA) and arachidonic acid (AA) levels were also significantly increased (Figure 2C). To check whether endogenously expressed DAGLs are responsible for the 2-AG production during differentiation, the cells were incubated with the dual DAGL inhibitor DH376. Cellular 2-AG and AA, but not AEA, levels were strongly reduced by DH376 (Figure 2D). The inhibitor also induced a significant delay in the differentiation of Neuro-2a cells, expressed as the fraction of neurite bearing cells after 24, 48, and 72 h of RA stimulation (Figure 2B). This suggested that DAGL-dependent 2-AG and/or AA production plays a role in the differentiation process, which is in line with the previous observations by Jung *et al.*[16].

To investigate which DAGL isoform is responsible for 2-AG production in Neuro-2a cells a genetic approach was used, because there are currently no subtype-specific DAGL inhibitors available. Of note, single cell heterogeneity (in 2-AG production and neurite outgrowth) prevented the unequivocal analysis of single cell clone knockouts (Supplementary Figure S1). Therefore, disruption of DAGLα and DAGLβ genes was performed by three sequential rounds of transfection of Cas9 and single guide RNA's (sgRNA) in Neuro-2a cell populations (Supplementary Figure S2A-C). This yielded three different Neuro-2a knockdown (KD) populations: DAGLα KD, DAGLβ KD and DAGLα–β KD. DAGLα and DAGLβ activity in these cell populations was measured using activity-based protein profiling (ABPP) to determine the efficiency of the genetic disruption. ABPP is a chemical proteomic method that uses chemical probes (e.g

fluorophosphonates (FP) or β-lactones) to assess the functional state of DAGLα and DAGLβ (and other serine hydrolases) in native biological systems. When coupled to fluorescent reporter groups, activity-based probes (ABPs) enable visualization of enzymatic activity in complex proteomes by sodium dodecyl sulfate polyacrylamide gel electrophoresis (SDS-PAGE) and in-gel fluorescence scanning. When coupled to a biotin reporter group, ABPs enable affinity enrichment and identification of enzyme activities by mass spectrometry (MS)-based proteomics. Gel-based ABPP with a fluorescent FP-probe (FP-TAMRA) and β-lactone probe MB064 showed a strong reduction (> 70%) of DAGLβ activity in the DAGLβ KD and DAGLα–β KD populations (Figure 3A-B), whereas other serine hydrolase activities were not affected. LC-MS-based chemical proteomics confirmed these findings (Figure 3C). Of note, no DAGLα activity was observed in either of the populations, including WT Neuro-2a (Figure 3A-B). The residual DAGLβ activity can be explained by a transfection efficiency below 100% and by insertion or deletion of a full codon upon Cas9-mediated DNA modification, thus preventing the frameshift that generally results in an early STOP-codon.

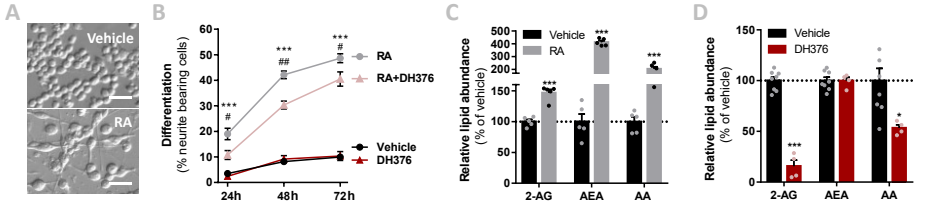

Figure 2 | RA-induced differentiation increased cellular 2-AG levels and is delayed by DH376 treatment. (A-C) Neuro-2a cells were differentiated with RA (50 µM, 2% serum, 24-72 h) in the presence or absence of inhibitor DH376 (100 nM). (A) Phase contrast microscopy of representative differentiated and non-differentiated Neuro-2a cultures (72 h incubation). Scale bar: 50 µm. (B) Neuro-2a differentiation was quantified as the percentage of neurite bearing cells (mean ± SEM (n=3), *t*-test: *** $p < 0.001$ vehicle versus RA, # $p < 0.05$, ## $p < 0.01$ RA versus RA-DH376). (C) Lipidomics analysis on vehicle and RA-stimulated cells (72 h). Lipid abundance was normalized to the number of cells. Data is expressed as % of vehicle (mean ± SEM (n=5), *t*-test: *** $p < 0.001$). (D) Lipidomics analysis on *in situ* DH376-treated Neuro-2a (100 nM, 2 h). Lipid abundance was normalized for the amount of protein. Data is expressed as % of vehicle (mean ± SEM (Veh: n=8, DH376: n=4), *t*-test: * $p < 0.05$, *** $p < 0.001$).

Next, the cellular 2-AG levels of these genetically modified Neuro-2a populations were determined using LC-MS. Surprisingly, despite having > 70% reduction in DAGLβ activity and no detectable DAGLα activity, the 2-AG levels in the DAGLα KD, DAGLβ KD or double DAGLα-β KD populations were not significantly different from WT populations (Figure 3C). To test whether the 2-AG production in the KD populations was still sensitive to DH376 treatment, the cells were incubated *in situ* with DH376 (100 nM, 2 h). Lipidomics analysis on these samples revealed that DH376 again abolished cellular 2-AG levels and reduced AA by 50% in all cell types (Figure 3C). Of note, a small but significant increase in AEA levels in the double DAGLα-β KD populations was observed (Figure 3C), which might be the result of increased ABHD4 activity (Figure 3D). Taken together, these data suggest that residual DAGLβ activity may be responsible for the entire pool of 2-AG,

which seems unlikely, or that an alternative, unidentified enzyme, which is sensitive to DH376, contributes to 2-AG biosynthesis in Neuro-2a cells.

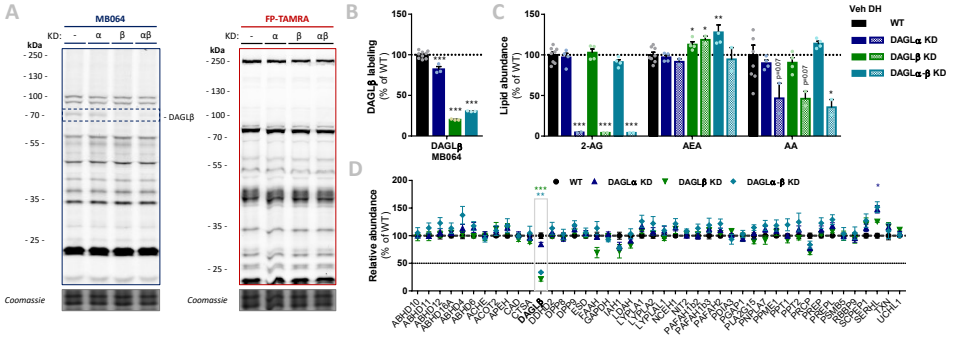

Figure 3 | DAGL KD did not alter 2-AG levels in Neuro-2a, whereas 2-AG was abolished by DAGL inhibitor DH376. (**A**-**B**) DAGL KD populations were analyzed by gel-based ABPP using probes MB064 (2 µM) and FP-TAMRA (500 nM) (20 min, rt). Coomassie served as protein loading control. (**B**) Probe labeling of DAGLβ was quantified and normalized for protein loading. Data is expressed as % of vehicle (mean ± SEM (WT: n=9, KD: n=3), *t*-test: *** $p < 0.001$). (**C**) Lipidomics analysis on WT and DAGL KD Neuro-2a populations treated *in situ* with vehicle or DH376 (100 nM, serum-free, 2 h). Lipid abundance was normalized for the amount of protein. Data is expressed as % of vehicle (mean ± SEM (WT: n=8, KD: n=4/2), *t*-test: * $p < 0.05$, ** $p < 0.01$, *** $p < 0.001$). (**D**) DAGL KD efficiency was assessed by chemical proteomics on WT and KD Neuro-2a cells using probes MB108 and FP-biotin (10 µM each, 30 min, 37 °C). Data is expressed as % of WT-vehicle (mean ± SEM (n=4), *t*-test with Holm-Sidak multiple comparison correction: * $p < 0.05$, ** $p < 0.01$, *** $p < 0.001$).

To identify all 2-AG producing enzymes targeted by DH376 in Neuro-2a, a chemical proteomics strategy was employed. The alkyne moiety of DH376 served as a ligation handle to introduce a reporter group via a copper(I)-catalyzed azide-alkyne cycloaddition ("click" chemistry)[19]. Neuro-2a cells were incubated with DH376, lysed and the covalently bound inhibitor-targets were conjugated to Cy5-azide, resolved by SDS-PAGE and visualized by in-gel fluorescence scanning (Figure 4A-B). Apart from DAGLβ, one other fluorescent band with a molecular weight of ~ 35 kDa was observed. Competitive ABPP using MB064 and FP-TAMRA suggested that this fluorescent band could be ABHD6, which was previously also reported as an off-target of DH376[4,20]. To confirm the identity of this protein in Neuro-2a cells, chemical proteomics was employed (Figure 4C). DAGLβ and ABHD6 were identified as the only targets of DH376 in Neuro-2a cells (Figure 4D). Thus, combined these data suggested that ABHD6 could be responsible for 2-AG production in conjunction with DAGLβ.

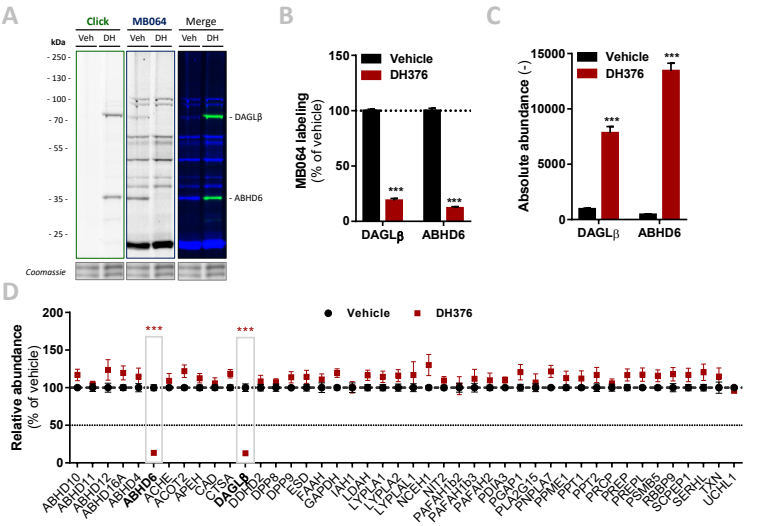

Figure 4 | DH376 targets DAGLβ and ABHD6 in Neuro-2a. Neuro-2a cells were treated *in situ* with vehicle or DH376 (100 nM, serum-free, 2 h) to investigate the DH376 interaction profile. (**A**, **B**) *In situ* DH376 targets were visualized by gel-based ABPP after conjugation of DH376 to Cy5-azide (5 µM, 60 min, rt) or with probe MB064 (2 µM, 20 min, rt). Coomassie served as a protein loading control. (**B**) Probe labeling was quantified and normalized for protein loading. Data is expressed as % of vehicle (mean ± SEM (Veh n=9, DH376 n=3), *t*-test: *** p < 0.001). (**C**) Chemical proteomics enabled DH376 target identification. Lysates of *in situ* DH376-treated Neuro-2a cells were conjugated to biotin-azide (40 µM, 60 min, 37 °C). Vehicle treated samples served as a negative control. Data is expressed as absolute abundance (mean ± SEM (n=4), *t*-test: *** p < 0.001). (**D**) Competitive proteomics validated ABHD6 and DAGLβ as DH376 targets in *in situ* treated Neuro-2a cells, using probes MB108 and FP-biotin (10 µM each, 30 min, 37 °C). Data is expressed as % of WT-Vehicle (mean ± SEM (n=4), *t*-test with Holm-Sidak multiple comparison correction: *** p < 0.001).

ABHD6 has previously been reported as a promiscuous lipase that not only uses 2-AG, but also various lysophosphatidyl species[21] and bis(monoacylglycero)phosphate[22] as substrates. Therefore, to confirm that ABHD6 can act also as a general lipase using DAG as a substrate, a DAG hydrolysis assay was developed based on fluorescent 1-nitrobenzoxadiazole-decanoyl-2-decanoyl-*sn*-glycerol (NBD-DAG) substrate. Lysates from human embryonic kidney 293-T (HEK293-T) cells overexpressing recombinant human ABHD6 (Figure 5A) or its catalytically inactive mutant (ABHD6^{S148A}) as a negative control, were incubated with NBD-DAG and analyzed by high performance thin layer chromatography (HPTLC). Lysates from HEK293-T cells expressing DAGLα or its catalytically inactive mutant (DAGLα^{S472A}) served as positive and negative controls respectively (Supplementary Figure S3A). Both DAGLα and ABHD6 exhibited DAG-lipase activity as their overexpression resulted in the hydrolysis of NBD-DAG, whereas their mutants did not (Figure 5B-C, Supplementary Figure S3C-D), thereby showing that ABHD6 is able to hydrolyze the *sn*-1 ester bond of an *sn*-1-acyl-2-decanoyl-glycerol. Of note, the NBD-DAG hydrolysis observed in HEK293-T cells expressing GFP reflects conversion of the substrate by endogenous hydrolases, including ABHD6 and to a lesser extent DAGLβ.

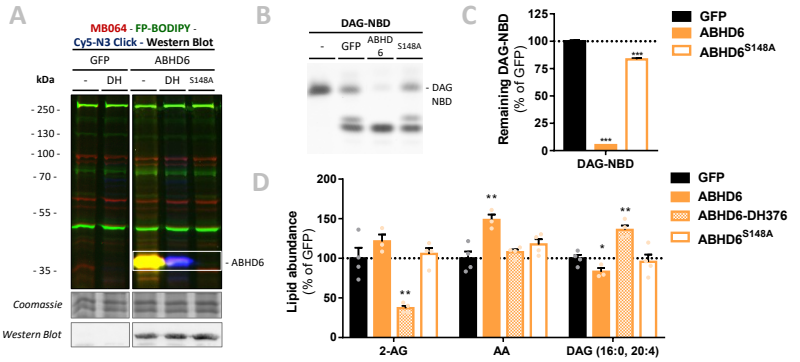

Figure 5 | Recombinant ABHD6 possesses DAG-lipase activity *in vitro* and *in situ*. HEK293-T cells were transiently transfected with GFP, ABHD6, or its catalytically inactive serine mutant (S148A) and treated *in situ* with vehicle or DH376 (DH, 1 µM, 2 h, serum-free). (**A**) Protein activity and expression was confirmed by gel-based ABPP and western blot. Samples were subsequently incubated with probes MB064 (red; 500 nM, 10 min, rt), FP-BODIPY (green; 500 nM, 10 min, rt), and Cy5-azide click mix (blue; 2.5 µM, 30 min, rt). Coomassie served as a protein loading control. Western blot with mouse-anti-FLAG (1:2500, 45 min, rt) verified expression of the catalytically inactive protein. (**B**-**C**) Whole cell lysates were incubated with DAG-NBD (5 µM, 30 min, 37 °C), lipids were extracted and analyzed by HPTLC. (**C**) DAG hydrolysis was quantified and expressed as % of GFP (mean ± SEM (n=3), *t*-test: *** $p < 0.001$). (**D**) Lipid abundance of transfected and *in situ* treated cells was measured and normalized to the amount of protein. Data is expressed as % of GFP-Vehicle (mean ± SEM (n=4), *t*-test: * $p < 0.05$, ** $p < 0.01$).

Next, it was determined whether ABHD6 could utilize endogenous DAGs in a cellular context. To this end, recombinant ABHD6 was overexpressed in HEK293-T cells (DAGLα as positive control and the catalytically inactive mutants as negative controls) and endogenous DAG (16:0, 20:4) levels were determined by targeted lipidomics (Figure 5D, Supplementary Figure S3D). Both ABHD6 and DAGLα overexpression reduced the levels of DAG (16:0, 20:4), whereas overexpression of the catalytically inactive mutants had no effect on the DAG-levels. DH376 treatment of the transfected cells prevented the reduction in DAG levels and even led to an increase in this lipid species, indicating that this DAG species serves also as an endogenous substrate for DAGLα/ABHD6. Overexpression of ABHD6 did not significantly affect 2-AG levels, in line with the dual MAG/DAG-lipase character of ABHD6, whereas its final product AA was increased (Figure 5D). In summary, these data indicate that ABHD6 is able to act as a DAG/MAG-lipase using DAG (16:0, 20:4) as an endogenous substrate.

To check whether endogenous cellular levels of 2-AG and AA are under control of ABHD6, a Neuro-2a ABHD6 KD population and a triple DAGLα-β-ABHD6 KD population were generated (Figure 6A, Supplementary Figure S2D-F). ABHD6 KD had no effects on 2-AG or AA levels (Figure 6C), which suggests that DAGLβ and ABHD6 can compensate for each other. The KD efficiency at the protein level was reduced in the triple DAGLα-DAGLβ-ABHD6 KD as compared to the single KDs as determined by gel-based ABPP (Figure 6A-B) and chemical proteomics (Figure 6D). It was estimated that approximately 40-50% of ABHD6 activity was remaining, as well as 30-40% DAGLβ activity. In line with the reduced ABHD6 and DAGL activity in the triple KD, both 2-AG and AA levels were reduced by approximately 30%.

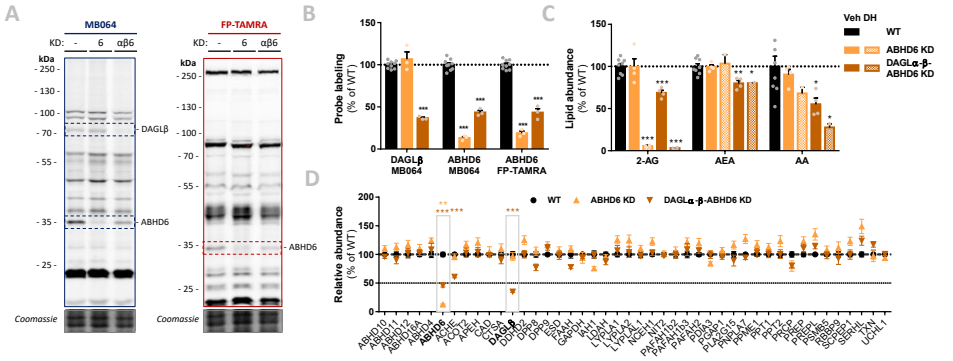

Figure 6 | Neuro-2a DAGLα-β-ABHD6 triple KD populations have decreased 2-AG levels. (**A**-**B**) ABHD6 and DAGLα-β-ABHD6 KD populations were analyzed by gel-based ABPP using probes MB064 (2 µM) and FP-TAMRA (500 nM) (20 min, rt). Coomassie served as a protein loading control. (**B**) Probe labeling was normalized for protein loading. Data is expressed as % of vehicle (mean ± SEM (WT: n=9, KD: n=3), *t*-test: *** $p < 0.001$). (**C**) Lipidomics analysis on WT and ABHD6 KD Neuro-2a populations treated *in situ* with vehicle or DH376 (100 nM, serum-free, 2 h). Lipid abundance was normalized for the amount of protein. Data is expressed as % of vehicle (mean ± SEM (WT: n=8, KD: n=4/2), *t*-test: * $p < 0.05$, ** $p < 0.01$, *** $p < 0.001$). (**D**) DAGL and ABHD6 KD efficiency was assessed by chemical proteomics on WT and KD Neuro-2a populations using probes MB108 and FP-biotin (10 µM each, 30 min, 37 °C). Data is expressed as % of WT-vehicle (mean ± SEM (n=4), *t*-test with Holm-Sidak multiple comparison correction: ** $p < 0.01$, *** $p < 0.001$).

Finally, in light of the finding that ABHD6 can act as a DAG lipase, the DAGLβ and ABHD6 activity in Neuro-2a cells during RA-induced differentiation was mapped by gel-based ABPP (Figure 7A). A threefold increase in ABHD6 activity was observed in differentiated Neuro-2a cells, whereas DAGLβ activity was decreased (Figure 7B). These data indicate that the RA-induced 2-AG and AA production (Figure 1B) in Neuro-2a cells is due to increased ABHD6 activity.

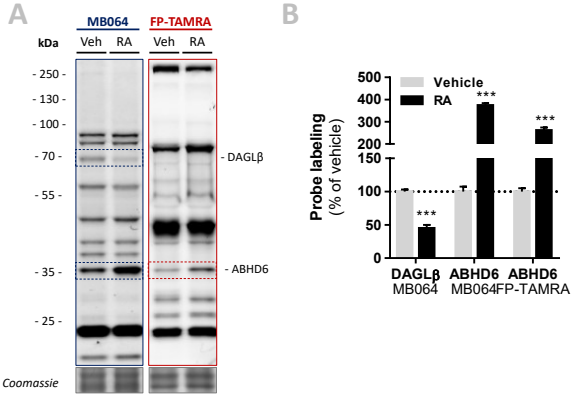

Figure 7 | DAGLβ activity decreased, while ABHD6 activity increased during RA-induced differentiation of Neuro-2a. Neuro-2a cells were stimulated by *in situ* treatment with retinoic acid (RA, 50 µM, 2% serum, 72 h). (**A**) Whole lysates of vehicle or RA stimulated cells were analyzed by gel-based ABPP using activity-based probes MB064 (2 µM) or FP-TAMRA (500 nM) (20 min, rt). Coomassie served as a protein loading control. (**B**) Probe labeling was normalized to loading control. Data is expressed as % of vehicle (mean ± SEM (n=3), *t*-test, *** $p < 0.001$).

Conclusion

DAGL-dependent endocannabinoid signaling is required for axonal growth and guidance in the developing brain. DAGLα and DAGLβ are reported as the main enzymes that produce the endocannabinoid 2-AG. It has been estimated that 10-20% of the 2-AG pool in mouse brain may result from alternative biosynthetic pathways. Here, ABHD6 is identified as an additional DAG lipase, which is supported by several lines of biochemical, genetic, and pharmacological evidence. First, genetic knockdown of both DAGLα and DAGLβ in Neuro-2a cells had no effect on cellular 2-AG levels. Second, the dual DAGL/ABHD6 inhibitor DH376 completely abolished cellular 2-AG levels. Third, ABHD6 catalyzed the degradation of a fluorescent DAG substrate. Fourth, overexpression of ABHD6, but not its catalytically inactive mutant, reduced endogenous DAG (16:0, 20:4) levels, which was inhibited by DH376. Fifth, cellular 2-AG levels decreased upon triple KD of DAGLα-β-ABHD6 in Neuro-2a. These data thus extend the role of ABHD6 from a MAG lipase to a DAG lipase and suggest a role for ABHD6 in neuronal differentiation.

Experimental procedures

Materials, probes, and inhibitors

Fluorophosphonate-rhodamine (FP-TAMRA) was purchased from Thermo Fisher, as well as synthesized in-house as previously described[23]. FP-Biotin was purchased from Santa Cruz Biotechnology. Fluorophosphonate-BODIPY (FP-BODIPY)[23], MB064[24], MB108[24], and DH376[4] were synthesized as previously described. All synthesized compounds were at least 95% pure and were analyzed by LC-MS, NMR, and HRMS. Primers were ordered from Sigma Aldrich or Integrated DNA Technologies. Other chemicals, reagents were purchased from Sigma Aldrich, unless indicated otherwise.

Cloning general

Full-length human DAGLα and ABHD6 cDNA (Source Bioscience) was cloned into the mammalian expression vector pcDNA3.1, containing ampicillin and neomycin resistance genes. The inserts were cloned in frame with a C-terminal FLAG-tag and site-directed mutagenesis was used to generate the catalytically inactive DAGLα^{S472A} and ABHD6^{S148A} mutants. pcDNA3.1 containing the gene for eGFP was used as a transfection control. Plasmids were isolated from transformed XL-10 Z-competent cells (Midi/Maxi Prep, Qiagen) and sequenced at the Leiden Genome Technology Center. Sequences were analyzed and verified (CLC Main Workbench).

Cell culture

General

Neuro-2a (murine neuroblastoma) and HEK293-T (human embryonic kidney) cells were cultured at 37 °C under 7% CO_2 in DMEM containing phenol red, stable glutamine, newborn bovine serum (10% v/v; Thermo Fisher), and penicillin and streptomycin (200 µg/mL each; Duchefa). Medium was refreshed every 2-3 days and cells were passaged twice a week at ~ 90% confluence by resuspension in fresh medium. Cell lines were purchased from ATCC and were regularly tested for mycoplasma contamination. Cultures were discarded after 2-3 months of use.

Single cell clone generation

Single cell clones of Neuro-2a cells were generated by seeding cells at a density of 0.5, 1, 2, or 4 cells per well in 96-wells plates. After several days, wells plates were screened for growth of single cell clones by phase-contrast microscopy (EVOS Auto FL2). Single cell clones were selected and expanded to full cultures.

Transient transfections (HEK293-T)

One day prior to transfection, HEK293-T cells were seeded at $1*10^6$ cells/well in 6-wells plates or at $0.3*10^6$ cells/well in 12-wells plates. Prior to transfection, culture medium was aspirated and a minimal amount of complete medium was added. A 3:1 (m/m) mixture of polyethyleneimine (PEI) and plasmid DNA (1.25 µg per 6-well, 0.625 µg per 12-well) was prepared in serum-free culture medium and incubated for 15 min at rt. Transfection was performed by dropwise addition of the PEI/DNA mixture to the cells. Transfection with pcDNA3.1 encoding GFP was used to generate control samples. 24 h Post-transfection culture medium was refreshed. *In situ* treatments were initiated 48 h post-transfection. Transfection efficiency was checked by fluorescence microscopy on eGFP transfected samples (EVOS FL2 Auto, GFP-channel).

In situ *treatments*

Neuro-2a cells were seeded at appropriate density (0.3*10^6 cells/well in 12-wells plates, 2.5*10^6 cells/dish in 6 cm dishes) 48 h prior to treatment. Alternatively, HEK293-T cells from transient transfections were used at 24-48 h post-transfection. Culture medium was aspirated and after a careful PBS wash, treatment medium (serum-free DMEM) containing vehicle (0.1% DMSO) or DH376 (100 nM – 1 µM, as indicated in figure legends) was added. After incubation for 2 h at 37 °C and 7% CO_2, treatment medium was aspirated and cells were carefully washed with PBS. Subsequently cells were harvested by resuspension in PBS and spun down (1000 *g*, 3 min, rt). Cell pellets were flash frozen in liquid nitrogen and stored at -80 °C until further use.

Retinoic acid stimulation

Neuro-2a cells were seeded at 1*10^5 cells/well in 6-well plates or 1*10^6 cells/ dish in 10 cm dishes. One day after seeding, medium was aspirated and retinoic acid stimulation was initiated by adding DMEM containing 2% newborn bovine serum and all-*trans*-retinoic acid (50 µM) or vehicle (0.1% DMSO). For Figure 2D, co-treatment was done with vehicle (0.1% DMSO) or DH376 (100 nM) throughout the entire differentiation process. After 24, 48 or 72 h of stimulation, neurite outgrowth was investigated using phase contrast microscopy (Olympus or EVOS FL2 Auto, phase contrast, large ring). Neurite outgrowth was quantified by counting the number of cells with a minimum of 2 outgrowth processes longer than the cell body, as a percentage of the total number of cells (3 dishes, 5 images per dish). Cell count and viability were checked by Trypan blue staining and automated cell counting (TC20™ Cell Counter, Bio-Rad).

CRISPR/Cas9-mediated knockdowns

Guide design & constructs

Two sgRNA's, in early exons, with high efficiency and specificity as predicted by CHOPCHOP v2 online web tool[25] (http://chopchop.cbu.uib.no) were selected. Guides were cloned into the BbsI restriction site of plasmid px330-U6-Chimeric_BB-CBh-hSpCas9 (gift from Feng Zhang, Addgene plasmid #42230) as previously described[26,27]. Constructs and primers are annotated in Table 1.

Knockdown population generation

Neuro-2a cells were transfected sequentially (3 times within the course of 10 days) to yield populations with a high knockdown efficiency. Cells were seeded at day 0, 3, and 6 and transfected at day 1, 4, and 7. Samples for T7E1 assays, and ABPP were harvested at day 2, 5, and 11 and after several weeks of culturing the cells. One day prior to the first transfection, Neuro-2a cells were seeded to a 6-well plate to reach 80% confluence at the time of transfection. Prior to transfection, culture medium was aspirated and 2 mL of fresh medium was added. A 5:1 (m/m) mixture of polyethyleneimine (PEI) (17.5 µg per well) and plasmid DNA (total 3.5 µg per well) was prepared in serum-free culture medium (250 µL each) and incubated (15 min, rt). Transfection was performed by dropwise addition of the PEI/DNA mixture to the cells. 24 h Post-transfection the culture medium was refreshed, a small amount of cells was harvested for analysis by T7E1 assay and ABPP, while the remainder was kept in culture under standard conditions for following transfections. After three transfection rounds, the cells were cultured according to standard protocol. Ampoules of knockdown populations were prepared (complete DMEM, 10% DMSO) and stored at -150 °C. Efficiency of knockdown was checked over time. Cells were discarded after 3 months of culture.

T7E1 assay

Genomic DNA was obtained by mixing 50 µL QuickExtract™ (Epicentre) with cell pellet (~ 10% of a well from a 6-well plate). The samples were incubated at 65 °C for 6 min, mixed by vortexing and then incubated at 98 °C for 2 min. Genomic DNA extracts were diluted in sterile water and directly used in PCR reactions. Genomic PCR reactions were performed on 2.5-5 µL isolated genomic DNA

extract using Phusion High-Fidelity DNA Polymerase (Thermo Fisher) in Phusion HF buffer Green (Thermo Fisher) in a final volume of 20 µL, for primers see Table 1.

For the T7E1 assay, genomic PCR products were denatured and reannealed in a thermocycler using the following program: 5 min at 95 °C, 95 to 85 °C using a ramp rate of -2 °C/s, 85 °C to 25 °C using a ramp rate of -0.2 °C/s. Annealed PCR product (8.5 µL) was mixed with NEB2 buffer (1 µL) and T7 endonuclease I (5 U, 0.5 µL; New England Biolabs), followed by a 30 min incubation at 37 °C. Digested PCR products were analyzed using agarose gel electrophoresis with ethidium bromide staining. A sample without T7 endonuclease I was taken along as control. Agarose gels were analyzed using ImageLab™ Software (Bio-Rad) and DNA modification efficiency was expressed as percentage T7E cleavage (volume integral of digested bands / volume integral all bands * 100%).

Table 1 | sgRNA targets, sgRNA oligos (top, bottom) and T7E1 primers (forward, reverse). Constructs indicated with an asterisk (*) were used to generate double and triple knockdowns.

sgRNA Target	Construct	Primer Sequences	
***Dagla* – Exon 2**	447*	Top:	CACCGAGGATTACAAACCTGCAGAG
		Bottom:	AAACCTCTGCAGGTTTGTAATCCTC
		Forward:	GAACTTGGGGTCTTTTTGTCTG
		Reverse:	CAAGGAAGAACAGGTAACCAGG
– Exon 3	485	Top:	CACCGCATGGCTGGCAGCTCTGGG
		Bottom:	AAACCCCAGAGCTGCCAGCCATGC
		Forward:	GGTAGTAGTTACTGCCGATGCC
		Reverse:	CTCTTCAGGGCTGACTCAGTTT
***Daglb* – Exon 1**	449*	Top:	CACCGTGGGAGGTGCGCCATGCCG
		Bottom:	AAACCGGCATGGCGCACCTCCCAC
		Forward:	TTAAACAGAAATGACCACACCG
		Reverse:	CCTGGTTTCTATGAATTGCTCC
– Exon 2	450	Top:	CACCGTGTATCTCACGCACAGAAGG
		Bottom:	AAACCCTTCTGTGCGTGAGATACAC
		Forward:	CTCCTACATCTCTTGCTTGCCT
		Reverse:	ACACAAATGGTAGCGCAGTATG
***Abhd6* – Exon 2**	724	Top:	CACCGGTTAACATGTTTGTGATTG
		Bottom:	AAACCAATCACAAACATGTTAACC
		Forward:	GATCCATGGTATACCCCTAACCACTGAGTCATCTC
		Reverse:	TGACTCGAGATTGGAATGGCGATATGGTTACACT
– Exon 3	725*	Top:	CACCAGTTCGCTACGCACACCATG
		Bottom:	AAACCATGGTGTGCGTAGCGAACT
		Forward:	TCCAAGCTTATGCCTGCTTGTTTGCTTTTATTT
		Reverse:	CAACACCGGTATCCTATGTTAGCTCACTCCCACCC

Whole lysate preparation

Cells were harvested in PBS and pelleted by centrifugation (1000 *g*, 3-5 min, rt). Cell pellets were snap-frozen and stored at -80 °C until further use. Cell pellets were thawed on ice, resuspended in cold lysis buffer (20 mM HEPES pH 7.2, 2 mM DTT, 250 mM sucrose, 1 mM $MgCl_2$, 2.5 U/mL benzonase) and incubated on ice (15-30 min). Protein concentrations were determined by a Quick Start™ Bradford Protein Assay (Bio-Rad). After dilution to 2 mg/mL in sucrose lysis buffer or storage buffer (20 mM HEPES pH 7.2, 2 mM DTT), samples were used or flash frozen in liquid nitrogen and stored at -80 °C until further use. DTT was left out of all buffers for samples intended for click-chemistry.

Activity-based protein profiling

Gel-based ABPP: Single probe

Whole lysate (2 mg/mL) was incubated with activity-based probes MB064 (250 nM - 2 µM, 20 min, rt) or FP-TAMRA (500 nM, 20 min, rt). The reaction was quenched with Laemmli buffer (30 min, rt) and 20 µg protein was resolved by SDS-PAGE (10% acrylamide gel) along with protein marker (PageRuler™ Plus, Thermo Fisher). In-gel fluorescence was detected in the Cy3- and Cy5-channel on a ChemiDoc™ MP imaging system (Bio-Rad) and gels were stained with coomassie after scanning. Fluorescence was quantified and normalized to coomassie staining using ImageLab™ software (Bio-Rad) and data was processed in Excel (Microsoft) and GraphPad Prism 7 (GraphPad).

Gel-based ABPP: Probe mixture

Whole lysates (DTT-free, 2 mg/mL) were incubated with activity-based probe MB064 (2 µM, 10 min, rt), followed by incubation with FP-TAMRA (500 nM, 10 min, rt) and a subsequent conjugation to Cy5-azide by incubation with click-mix (2.5/10 µM Cy5-N_3, 67 mM sodium ascorbate, 4 mM $CuSO_4 \cdot (H_2O)_5$, 1.3 mM THPTA; 30 min, rt). The reaction was quenched with Laemmli buffer (30 min, rt) and 15 µg protein was resolved by SDS-PAGE (10% acrylamide gel) along with protein marker (PageRuler™ Plus, Thermo Fisher). In-gel fluorescence was detected in the Cy3- and Cy5-channel on a ChemiDoc™ MP imaging system (Bio-Rad) and gels were stained with coomassie after scanning. Fluorescence was quantified and normalized to coomassie staining using ImageLab™ software (Bio-Rad) and data was processed in Excel (Microsoft) and GraphPad Prism 7 (GraphPad).

Chemical proteomics with label-free quantification

The chemical proteomics workflow was modified from a previously published protocol[20]. In short, for general profiling of the serine hydrolases the whole lysates (250 µg protein, n=4) were incubated with serine hydrolase probe cocktail (10 µM MB108, 10 µM FP-Biotin, 30 min, 37 °C, 300 rpm). A denatured protein sample (1% SDS, 5 min, 100 ˚C) was taken along as a negative control. For DH376 target identification, the whole lysates of DH376 treated cells (250 µg protein, n=4) were conjugated to biotin-azide by the addition of 10x concentrated click mix (final: 1 mM $CuSO_4(H_2O)_5$, 0.56 mM sodium ascorbate, 0.2 mM THPTA, 0.04 mM biotin-azide in MilliQ) and subsequent incubation (60 min, 37 °C, 300 rpm). A vehicle treated sample was taken along as a negative control. Precipitation, alkylation, avidin enrichment, on-bead digestion and sample preparation was performed according to protocol[20]. Dried peptides were stored at -20 °C until LC-MS analysis. Prior to measurement, samples were reconstituted in 50 µL LC-MS solution and transferred to LC-MS vials. Analysis was performed using Progenesis QIP (Waters) as published, using the following cut-offs: ≥ 2-fold enrichment compared to negative control, ≥ 2 peptides, ≥ 1 unique peptide, peptide ion correlations ≥ 0.7.

Lipidomics

Sample preparation: Neuro-2a retinoic acid stimulation

Neuro-2a cells were seeded at $0.75*10^6$ cells/dish in a 10 cm dish. One day after seeding, medium was aspirated and retinoic acid stimulation was initiated by adding DMEM containing 2% serum and retinoic acid (50 µM) or vehicle (0.1% DMSO). After 72 h neurite outgrowth was investigated using phase contrast microscopy (Olympus). Cells were carefully washed with PBS and harvested by resuspension in PBS (for retinoic acid stimulated cells, 5 dishes were combined to yield sufficient cells). Cells were pelleted (200 *g*, 10 min, rt) and resuspended in 1 mL PBS. Cell count and viability were checked by Trypan blue staining and automated cell counting (TC20™ Cell Counter, Bio-Rad) and $2*10^6$ cells were pelleted (1000 *g,* 3 min, rt). Pellets were flash frozen in liquid nitrogen and stored at -80 °C until lipid extraction.

Sample preparation: Neuro-2a single cell clones

Neuro-2a cells were seeded at $1.25*10^6$ cells/ dish in a 10 cm dish. One day after seeding, medium was aspirated and cells were cultured in 2% serum and vehicle (0.1% DMSO). After 48 h cells were carefully washed with PBS and harvested by resuspension in. Cells were pelleted (200 *g*, 5 min, rt) and resuspended in PBS. Cell count and viability were checked by Trypan blue staining and automated cell counting (TC20™ Cell Counter, Bio-Rad) and $1*10^6$ cells were pelleted (1000 *g,* 3 min, rt). Pellets were flash frozen in liquid nitrogen and stored at -80 °C until lipid extraction.

Sample preparation: Neuro-2a knockdown populations

Neuro-2a cells were seeded at $2.5*10^6$ cells/dish in a 6 cm dish 48 h prior to treatment. Alternatively, HEK293-T cells from transient transfections were used at 48 h post-transfection (6-wells format). Culture medium was aspirated and after a careful PBS wash, treatment medium (serum-free DMEM) containing vehicle (0.1% DMSO) or DH376 (100 nM) was added. After incubation for 2 h at 37 °C and 7% CO_2, treatment medium was aspirated and cells were carefully washed with PBS. Subsequently cells were harvested by resuspension in 1250 µL PBS. Cell count and viability were checked by Trypan blue staining and automated cell counting (TC20™ Cell Counter, Bio-Rad). Cells from 1000 µL suspension were spun down (1000 *g*, 3 min, rt) in a low binding Eppendorf tube. Pellets were flash frozen in liquid nitrogen and stored at -80 °C until lipid extraction. The remaining cell suspension (~ 200 µL) was flash frozen and used to determine the protein concentration of each sample. The suspension was thawed on ice and cells were lysed by sonication using a probe sonicator (Heidolph; 5 s per sample, 10% amplitude). Protein concentrations (~ 1 mg/mL) were determined by a Quick Start™ Bradford Protein Assay (Bio-Rad) and were used for normalization of the lipid abundance.

Lipid extraction

Lipid extraction was performed as previously described[28] with minor adaptations. In brief, cell pellets were transferred into 1.5 mL Eppendorf tubes, spiked with 10 µL of deuterated internal standard mix (Table 2), followed by addition of 200 µL of ammonium acetate buffer (0.1 M, pH 4) was added. After addition of 1000 µL methyl *tert*-butyl ether (MTBE), the tubes were thoroughly mixed for 5 min using a bullet blender (Next Advance) at medium speed, followed by a centrifugation step (16,000 *g*, 5 min, 4 °C). Then 850 µL of the upper MTBE layer was transferred to clean 1.5 mL Eppendorf tubes. Samples were dried in a SpeedVac (Eppendorf) followed by reconstitution in 50 µL of acetonitrile:water (90:10, v/v). The reconstituted samples were centrifuged (16,000 *g*, 3 min, 4 °C) before transferring into LC-MS vials. 5 µL of each sample was injected into the LC-MS/MS system.

General LC-MS/MS Analysis

LC-MS/MS analysis was performed as previously described[28] with minor adaptations. A targeted analysis of 31 compounds, including endocannabinoids and related *N*-acylethanolamines (NAEs) and free fatty acids (Table 2), was measured using an Acquity UPLC I class Binary solvent manager pump (Waters) in conjugation with AB SCIEX 6500 quadrupole-ion trap (AB Sciex). The separation was performed with an Acquity HSS T3 column (2.1 × 100 mm, 1.8 µm) maintained at 45 °C. The aqueous mobile phase A consisted of 2 mM ammonium formate and 10 mM formic acid, and the organic mobile phase B was acetonitrile. The flow rate was set to 0.55 mL/min; initial gradient conditions were 55% B held for 2 min and linearly ramped to 100% B over 6 min and held for 2 min; after 10 s the system returned to initial conditions and held 2 min before next injection. Electrospray ionization-MS and a selective Multiple Reaction Mode (sMRM) was used for endocannabinoid quantification. Individually optimized MRM transitions using their synthetic standards for target compounds and internal standards are described in Table 2.

DAG Analysis

LC-MS/MS analysis of DAG (16:0, 20:4) was performed as described in the above section with the following adaptations. The mobile phase A was 10 mM ammonium formate and 10 mM formic acid in 60:40 (v/v%) acetonitrile:water, the mobile phase B was 10 mM ammonium formate and 10 mM formic acid in 10:90 (v/v%) acetonitrile:isopropanol. The flow rate was set to 0.4 mL/min; initial gradient conditions were 50% B for 0.5 min and linearly ramped to 60% B at 2 min, then ramped to 90% B at 6 min; after 6 seconds the system returned to initial conditions and held 1.4 min before next injection.

Table 2 | LC-MS Standards and internal standards for lipidomics analysis.

Standards				
Abbreviation	Metabolite	Q1	Q3	Polarity
DAG (16:0, 20:4)	1-Palmitoyl-2-arachidonoyl-sn-glycerol	634	313	+
1&2-AG	2&1-Arachidonoylglycerol (20:4)	379	287	+
AEA	Anandamide (20:4)	348	62	+
DHEA	*N*-Docosahexaenoylethanolamide (22:6)	372	62	+
LEA	*N*-Linoleoylethanolamide (18:2)	324	62	+
NADA	*N*-Arachidonoyl dopamine (28:4)	440	137	+
OEA	*N*-Oleoylethanolamide (18:1)	326	62	+
PEA	*N*-Palmitoylethanolamide (16:0)	300	62	+
SEA	*N*-Stearoylethanolamide (18:0)	328	62	+
2-AGE	2-Arachidonyl glycerol ether (20:4)	365	273	+
DEA	*N*-Docosatetraenoylethanolamide (22:4)	376	62	+
DGLEA	Dihomo-γ-Linolenoyl Ethanolamide (18:3)	350	62	+
O-AEA	*O*-Arachidonoyl ethanolamine (20:4)	348	62	+
2-LG	2-Linoleoyl glycerol (18:2)	355	263	+
1-LG	1-Linoleoyl glycerol (18:2)	355	263	+
2-OG	2-Oleoyl glycerol (18:1)	357	265	+
EPEA	Eicosapentaenoyl ethanolamide (20:5)	346	62	+
POEA	*N*-Palmitoleoylethanolamide (16:1)	298	62	+
ETAEA	Eicosatrienoic acid ethanolamide (20:3)	350	62	+
PDEA	*N*-Pentadecanoylethanolamide (15:0)	286	62	+
α-LEA	*N*-α-Linolenylethanolamide (18:2)	322	62	+
OA	Oleic acid (18:1)	281	263	-
LA	Linoleic acid (18:2-ω6)	279	261	-
α-LA	α-Linolenic acid (18:3-ω3)	277	233	-
γ-LA	γ-Linolenic acid (18:3-ω6)	277	233	-
DGLA	Dihomo-γ-linolenic acid (20:3-ω6)	305	261	-
MA	Mead acid (20:3-ω9)	305	261	-
AA	Arachidonic Acid (20:4-ω6)	303	259	-
EPA	Eicosapentaenoic acid (20:5-ω3)	301	257	-
DTA	Docosatetraenoic acid (22:4-ω6)	332	288	-
DHA	Docosahexaenoic acid (22:6-ω3)	327	283	-
Internal standards				
Abbreviation	Metabolite	Q1	Q3	Polarity
DAG (34:0)	1-Margaroyl-2-margaroyl-sn-glycerol	614	327	+
2-AG (20:4)-d8	2-Arachidonoylglycerol-d8	387	294	+
PEA (16:0)-d4	Palmitoyl ethanolamide-d4	304	62	+
SEA (18:0)-d3	Stearoyl ethanolamide-d3	331	62	+
OEA (18:1)-d4	Oleoyl ethanolamide-d4	330	66	+
LEA (18:2)-d4	Linoleoyl ethanolamide-d4	328	66	+
AEA (20:4)-d8	Arachidonoyl ethanolamide-d8	356	62	+
DHEA (22:6)-d4	Docosahexaenoyl ethanolamide-d4	376	66	+
NADA (28:4)-d8	*N*-Arachidonoyl dopamine-d8	448	137	+

NBD-HPTLC assay

Whole lysates of HEK293-T transiently expressing eGFP (control), DAGLα, ABHD6 or their catalytically inactive serine mutants were prepared as described above. Lysate (100 µg protein) was mixed with 5 µM DAG-NBD (Cayman Chemical; 2 mM stock in EtOH) in HEPES buffer (20 mM HEPES pH7.2, 2 mM DTT) and incubated (30 min, 37 °C, 600 rpm, dark). As a control, a sample without protein was taken along. After incubation, lipids were extracted by a Bligh and Dyer extraction. In short, 800 µL chloroform:methanol (1:1, v/v) and 110 uL MilliQ were added to the sample. Phases were separated by centrifugation (5 min, 13,000 *g*) and the bottom layer was transferred to a dark Eppendorf tube. The upper layer was extracted once more by adding 400 µL chloroform. The lipid extract was dried in a speedvac (Eppendorf) (45 min, 45 °C). Lipids were reconstituted in 40 µL methanol, and lipids (2 µL, n=3) were separated by thin layer chromatography on HPTLC Silica gel 60 plates (Merck) using chloroform:methanol (80:20, v/v) as eluent. NBD-labeled lipids were detected using a Typhoon Imaging system (GE Heatlhcare Bio-Science) (Alexa488 channel, 250V). Fluorescence was quantified using ImageLab™ software (Bio-Rad). Excel (Microsoft) and GraphPad Prism 7 (GraphPad) were used for further analysis. DAG-NBD was expressed as fraction of the total NBD intensity in each lane and normalized to eGFP samples.

Western blot

Cell lysates were denatured with Laemmli buffer (30 min, rt) and 20 µg lysate was resolved on a 10% acrylamide SDS-PAGE gel along with PageRuler™ Plus Protein Marker (Thermo Scientific). Proteins were transferred to 0.2 µm polyvinylidene difluoride membranes by Trans-Blot Turbo™ Transfer system (Bio-Rad). Membranes were washed with TBS (50 mM Tris, 150 mM NaCl) and blocked with 5% milk in TBS-T (50 mM Tris, 150 mM NaCl, 0.05% Tween 20) (1 h, rt). Membranes were then incubated with primary antibody mouse-anti-FLAG (F3156, Sigma Aldrich; 1:2500 in 5% milk in TBS-T, 45 min, rt) washed with TBS-T, incubated with secondary donkey-anti-mouse-Alexa647 (A-31571, Thermo Fisher; 1:10000 in 5% milk TBS-T, 45 min, rt), and washed with TBS-T and TBS. Fluorescence was detected on the ChemiDoc™ MP imaging system (Bio-Rad) in the Alexa647 channel, and Cy3/Cy5 channels for the protein marker. Signal was normalized to coomassie staining using ImageLab™ software (Bio-Rad) and data was processed in Excel (Microsoft) and GraphPad Prism 7 (GraphPad).

Statistical methods

All statistical measures and methods are included in the respective figure or table captions. In brief: all data are shown as the mean ± SEM, unless indicated otherwise. A Student's *t*-test (two-tailed, unpaired) was used to determine statistical significance, with a Holm-Sidak multi-comparison correction for proteomics data using GraphPad Prism 7 (GraphPad). Samples were compared to WT/Vehicle/GFP controls and statistical significance is indicated as * $p < 0.05$, ** $p < 0.01$, *** $p < 0.001$.

Supplementary data

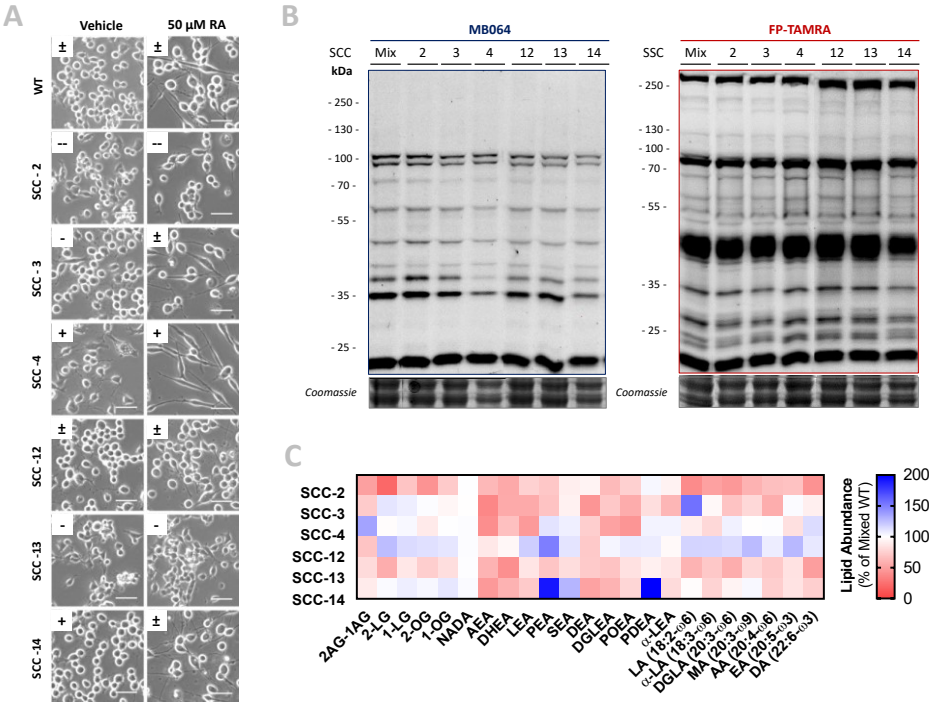

Figure S1 | Neuro-2a single cell clones have diverging phenotypes and lipid profiles. (**A**) Neuro-2a and Neuro-2a single cell clones (SCCs) show a diverging extent of neurite outgrowth upon treatment with retinoic acid (50 µM, 0.1% DMSO, 2% serum, 48 h). -/±/+ indicate the state of neurite outgrowth as compared to the mixed culture under the same conditions. Scale bar: 50 µm. (**B**) WT Neuro-2a and six different WT Neuro-2a single cell clones (SCCs) were analyzed by gel-based ABPP using probes MB064 (250 nM) and FP-TAMRA (500 nM) (20 min, rt). Coomassie served as a protein loading control. (**C**) Heat map summary of lipidomics performed on Neuro-2a and Neuro-2a SCCs revealed variation in lipid abundance between clones. Lipid abundance was normalized to cell number and data is expressed as % of WT (n=3).

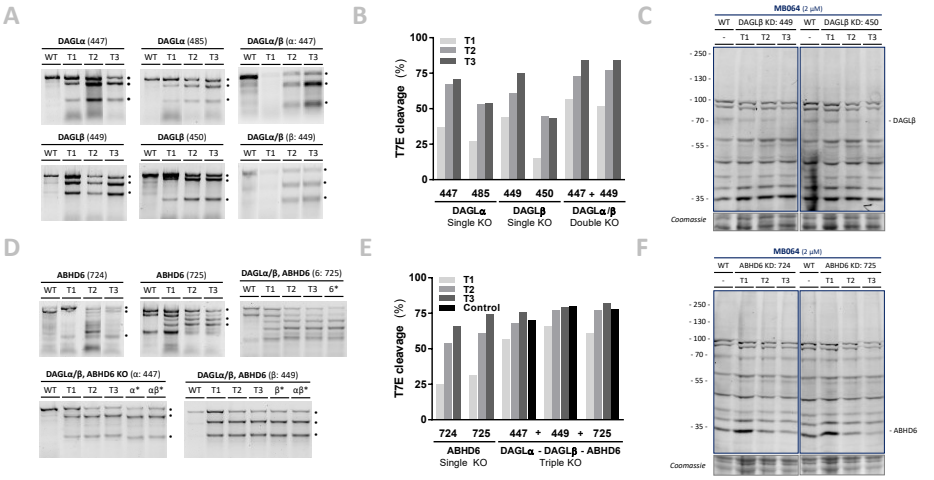

Figure S2 | Efficiency of CRISPR/Cas9-mediated knockdown in Neuro-2a. Knockdown populations were generated by three sequential transfections (T1-T3) with Cas9 and two different separate guides for each target. Most efficient guides were used to generate double and triple knockdowns. (**A**-**B**, **D**-**E**) Knockdown efficiency is determined by a T7E1 assay on genomic DNA was analyzed after each round of transfection and quantified for DAGL (**A**-**B**) and ABHD6 (**D**-**E**) knockdowns. (**C**, **F**) ABPP analysis of knockdown efficiency. After each transfection, whole lysates were incubated with MB064 (2 μM, 20 min, rt) and analyzed by SDS-PAGE.

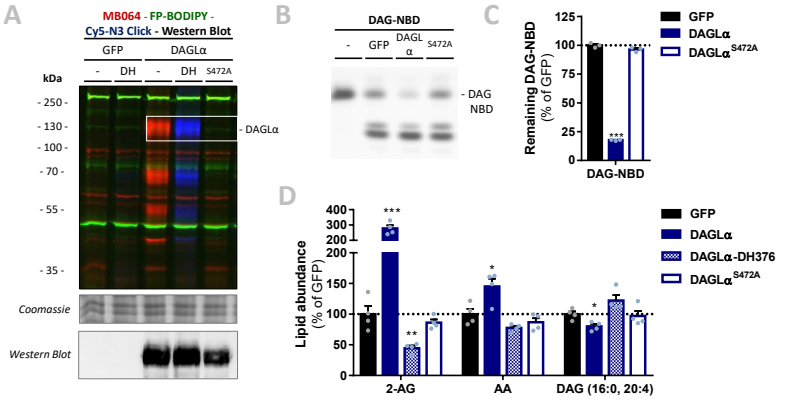

Figure S3 | Recombinant DAGLα possesses DAG-lipase activity *in vitro* and *in situ*. HEK293-T cells were transiently transfected with GFP, DAGLα or its catalytically inactive serine mutants (S472A) and treated *in situ* with vehicle or DH376 (DH, 1 μM, 2 h, serum-free). (**A**) Protein activity and expression were confirmed by gel-based ABPP and western blot. Samples were subsequently incubated with probes MB064 (500 nM, 10 min, rt), FP-BODIPY (500 nM, 10 min, rt), and Cy5-azide click mix (2.5 μM, 30 min, rt). Coomassie served as a protein loading control. Western blot with mouse-anti-FLAG (1:2500, 45 min, rt) verified expression of the catalytically inactive protein. (**B**-**C**) Whole lysates were incubated with DAG-NBD (5 μM, 30 min, 37 °C, 600 rpm). Lipids were extracted and analyzed by HPTLC (n=3). DAG hydrolysis was quantified and expressed as % of GFP (mean ± SEM (n=3), *t*-test: *** $p < 0.001$). (**D**) Lipid abundance of transfected and *in situ* treated cells was measured and normalized to the amount of protein (n=4). Data is expressed as % of GFP-Vehicle (mean ± SEM (n=4), *t*-test: * $p < 0.05$, ** $p < 0.01$, *** $p < 0.001$).

References

1. Di Marzo, V. Endocannabinoid signaling in the brain: biosynthetic mechanisms in the limelight. *Nat. Neurosci.* **14,** 9–15 (2011).
2. Bisogno, T. *et al.* Cloning of the first sn1-DAG lipases points to the spatial and temporal regulation of endocannabinoid signaling in the brain. *J. Cell Biol.* **163,** 463–468 (2003).
3. Gao, Y. *et al.* Loss of Retrograde Endocannabinoid Signaling and Reduced Adult Neurogenesis in Diacylglycerol Lipase Knock-out Mice. *J. Neurosci.* **30,** 2017–2024 (2010).
4. Ogasawara, D. *et al.* Rapid and profound rewiring of brain lipid signaling networks by acute diacylglycerol lipase inhibition. *Proc. Natl. Acad. Sci.* **113,** 26–33 (2016).
5. Deng, H. *et al.* Triazole Ureas Act as Diacylglycerol Lipase Inhibitors and Prevent Fasting-Induced Refeeding. *J. Med. Chem.* **60,** 428–440 (2017).
6. McReynolds, J. R. *et al.* Stress Promotes Drug Seeking Through Glucocorticoid-Dependent Endocannabinoid Mobilization in the Prelimbic Cortex. *Biol. Psychiatry* **84,** 85–94 (2018).
7. Bluett, R. J. *et al.* Endocannabinoid signalling modulates susceptibility to traumatic stress exposure. *Nat. Commun.* **8,** 14782 (2017).
8. Dinh, T. P., Freund, T. F. & Piomelli, D. A role for monoglyceride lipase in 2-arachidonoylglycerol inactivation. in *Chemistry and Physics of Lipids* **121,** 149–158 (2002).
9. Marrs, W. R. *et al.* The serine hydrolase ABHD6 controls the accumulation and efficacy of 2-AG at cannabinoid receptors. *Nat. Neurosci.* **13,** 951–7 (2010).
10. Blankman, J. L., Simon, G. M. & Cravatt, B. F. A comprehensive profile of brain enzymes that hydrolyze the endocannabinoid 2-arachidonoylglycerol. *Chem. Biol.* **14,** 1347–1356 (2007).
11. Savinainen, J. R., Saario, S. M. & Laitinen, J. T. The serine hydrolases MAGL, ABHD6 and ABHD12 as guardians of 2-arachidonoylglycerol signalling through cannabinoid receptors. *Acta Physiologica* **204,** 267–276 (2012).
12. Oudin, M. J., Hobbs, C. & Doherty, P. DAGL-dependent endocannabinoid signalling: Roles in axonal pathfinding, synaptic plasticity and adult neurogenesis. *European Journal of Neuroscience* **34,** 1634–1646 (2011).
13. Harkany, T. *et al.* The emerging functions of endocannabinoid signaling during CNS development. *Trends in Pharmacological Sciences* **28,** 83–92 (2007).
14. Watson, S., Chambers, D., Hobbs, C., Doherty, P. & Graham, A. The endocannabinoid receptor, CB1, is required for normal axonal growth and fasciculation. *Mol. Cell. Neurosci.* **38,** 89–97 (2008).
15. Wu, C. S. *et al.* Requirement of cannabinoid CB1receptors in cortical pyramidal neurons for appropriate development of corticothalamic and thalamocortical projections. *Eur. J. Neurosci.* **32,** 693–706 (2010).
16. Jung, K.-M., Astarita, G., Thongkham, D. & Piomelli, D. Diacylglycerol lipase-alpha and -beta control neurite outgrowth in neuro-2a cells through distinct molecular mechanisms. *Mol. Pharmacol.* **80,** 60–7 (2011).
17. Oudin, M. J. *et al.* Endocannabinoids Regulate the Migration of Subventricular Zone-Derived Neuroblasts in the Postnatal Brain. *J. Neurosci.* **31,** 4000–4011 (2011).
18. Berghuis, P. *et al.* Hardwiring the bain: Endocannabinoids shape neuronal connectivity. *Science* **316,** 1212–1216 (2007).
19. Rostovtsev, V. V., Green, L. G., Fokin, V. V. & Sharpless, K. B. A stepwise huisgen cycloaddition process: Copper(I)-catalyzed regioselective 'ligation' of azides and terminal alkynes. *Angew. Chemie - Int. Ed.* **41,** 2596–2599 (2002).
20. van Rooden, E. J. *et al.* Mapping in vivo target interaction profiles of covalent inhibitors using chemical proteomics with label-free quantification. *Nat. Protoc.* **13,** 752–767 (2018).
21. Thomas, G. *et al.* The Serine Hydrolase ABHD6 Is a Critical Regulator of the Metabolic Syndrome. *Cell Rep.* **5,** 508–520 (2013).

22. Pribasnig, M. A. *et al.* α/β hydrolase domain-containing 6 (ABHD6) degrades the late Endosomal/Lysosomal lipid Bis(Monoacylglycero)phosphate. *J. Biol. Chem.* **290,** 29869–29881 (2015).
23. Janssen, A. P. A. *et al.* Development of a Multiplexed Activity-Based Protein Profiling Assay to Evaluate Activity of Endocannabinoid Hydrolase Inhibitors. *ACS Chem. Biol.* **13,** 2406–2413 (2018).
24. Baggelaar, M. P. *et al.* Development of an activity-based probe and in silico design reveal highly selective inhibitors for diacylglycerol lipase-α in brain. *Angew. Chemie - Int. Ed.* **52,** 12081–12085 (2013).
25. Labun, K., Montague, T. G., Gagnon, J. A., Thyme, S. B. & Valen, E. CHOPCHOP v2: a web tool for the next generation of CRISPR genome engineering. *Nucleic Acids Res.* **44,** W272–W276 (2016).
26. Ran, F. A. *et al.* Genome engineering using the CRISPR-Cas9 system. *Nat Protoc* **8,** 2281–2308 (2013).
27. Cong, L. *et al.* Multiplex genome engineering using CRISPR/Cas systems. *Science* **339,** 819–823 (2013).
28. Van Esbroeck, A. C. M. *et al.* Activity-based protein profiling reveals off-target proteins of the FAAH inhibitor BIA 10-2474. *Science* **356,** 1084–1087 (2017).